Enhancing the Activity of a β-Helical Antifreeze Protein by the Engineered Addition of Coils†

Christopher B. Marshall,‡ Margaret E. Daley,§ Brian D. Sykes,§ and Peter L. Davies*,‡

Department of Biochemistry and Protein Engineering Network Centres of Excellence, Queen's University, Kingston, Ontario, Canada K7L 3N6, and Department of Biochemistry and Protein Engineering Network Centres of Excellence, University of Alberta, Edmonton, Alberta, Canada T6G 2H7

Received May 31, 2004; Revised Manuscript Received July 12, 2004

ABSTRACT: The effectiveness of natural antifreeze proteins in inhibiting the growth of a seed ice crystal seems to vary with protein size. Here we have made use of the extreme regularity of the β-helical antifreeze protein from the beetle *Tenebrio molitor* to explore systematically the relationship between antifreeze activity and the area of the ice-binding site. Each of the 12-amino acid, disulfide-bonded central coils of the β-helix contains a Thr-Xaa-Thr ice-binding motif. By adding coils to, and deleting coils from, the seven-coil parent antifreeze protein, we have made a series of constructs with 6−11 coils. Misfolded forms of these antifreezes were removed by ice affinity purification to accurately compare the specific activity of each construct. There was a 10−100-fold gain in activity upon going from six to nine coils, depending on the concentration that was compared. Activity was maximal for the nine-coil construct, which gave a freezing point depression of 6.5 C° at 0.7 mg/mL, but actually decreased for the 10- and 11-coil constructs. This small loss in activity might result from the accumulation of a slight mismatch between the spacing of the ice-binding threonine residues and the O atoms of the ice lattice.

A number of cold-adapted species produce antifreeze proteins (AFPs),[1] which help to protect these organisms from damage induced by uncontrolled ice growth at sub-zero temperatures (*1*−*3*). There are several different types of AFPs, which are not homologous and are diverse in sequence and structure, but appear to function through a common mechanism (*4*−*7*). AFPs adsorb to the surface of ice such that the addition of water molecules to the lattice is limited to the area between bound AFPs (*8*, *9*). This forces the ice to grow in locally curved fronts, a process that is thermodynamically disfavored and requires lower temperatures. In effect, the nonequilibrium freezing temperature is depressed below the colligative melting temperature. The difference between these temperatures can be measured and is termed thermal hysteresis (TH).

The several distinct types of AFPs can be categorized into two groups on the basis of repetition (*6*). The amino acid sequences and structures of the repetitive AFPs are comprised of repeating elements that complement the regularity of the structure of the ice lattice. The type I AFPs produced by flounders (and sculpins) are long α-helices comprised of 11-amino acid repeats, each of which forms three helical turns, positioning residues that interact with ice on one face of the helix (*10*).

The two different insect AFPs that have been structurally characterized are also repetitive. The spruce budworm AFP is a left-handed β-helix composed of tandem 15-amino acid imperfect repeats that form a triangular cross section and present a regular array of Thr residues on a flat β-sheet on the surface of the protein (*11*, *12*). The AFP produced by the beetle *Tenebrio molitor* is a right-handed β-helix comprised of 12-amino acid repeats that stack to form a rectangular "box" with an array of Thr residues on the surface (Figure 1b) (*13*, *14*). In each case, the distances between Thr residues in the array match the spacing of oxygen atoms in the ice lattice, and the Thr array has been demonstrated to be the ice-binding face of the protein (*11*, *15*).

The nonrepetitive AFPs that have been structurally characterized are small globular proteins but may have a relatively flat surface that interacts with ice. Type II AFPs, which are produced by smelts, herring, and sea raven, are homologous to the sugar-binding domain of Ca^{2+}-dependent (C-type) lectins (*16*). Type III AFPs, which are produced by eel pouts, are homologous to the C-terminal domain of sialic acid synthase (*17*). A number of lines of evidence indicate that the activity of an AFP increases with an increase in the size of the protein. For the nonrepetitive type III AFP, creating fusion proteins with other domains increases the total size of the protein and substantially enhances activity (*18*).

† Supported by Grant 6199 from the Canadian Institutes of Health Research (CIHR) (to P.L.D.) and by Grant ENG1 from the Protein Engineering Network of Centres of Excellence (PENCE) (to P.L.D. and B.D.S.). B.D.S. holds a Canada Research Chair in Structural Biology and P.L.D. a Canada Research Chair in Protein Engineering. C.B.M. is supported by an Ontario Graduate Scholarship in Science and Technology and M.E.D. by a CIHR Doctoral Research Award.

* To whom correspondence should be addressed: Department of Biochemistry, Queen's University, Kingston, Ontario, Canada K7L 3N6. E-mail: daviesp@post.queensu.ca. Telephone: (613) 533-2983. Fax: (613) 533-2497.

‡ Queen's University.

§ University of Alberta.

[1] Abbreviations: AFP, antifreeze protein; D, deuterium; HPLC, high-performance liquid chromatography; IAP, ice affinity purification; NMR, nuclear magnetic resonance; Osm, osmol; sbw, spruce budworm; TH, thermal hysteresis; Tm, *Tenebrio molitor*; TOCSY, total correlation spectroscopy; wt, wild-type.

10.1021/bi0488909 CCC: $27.50
Published on Web 08/25/2004

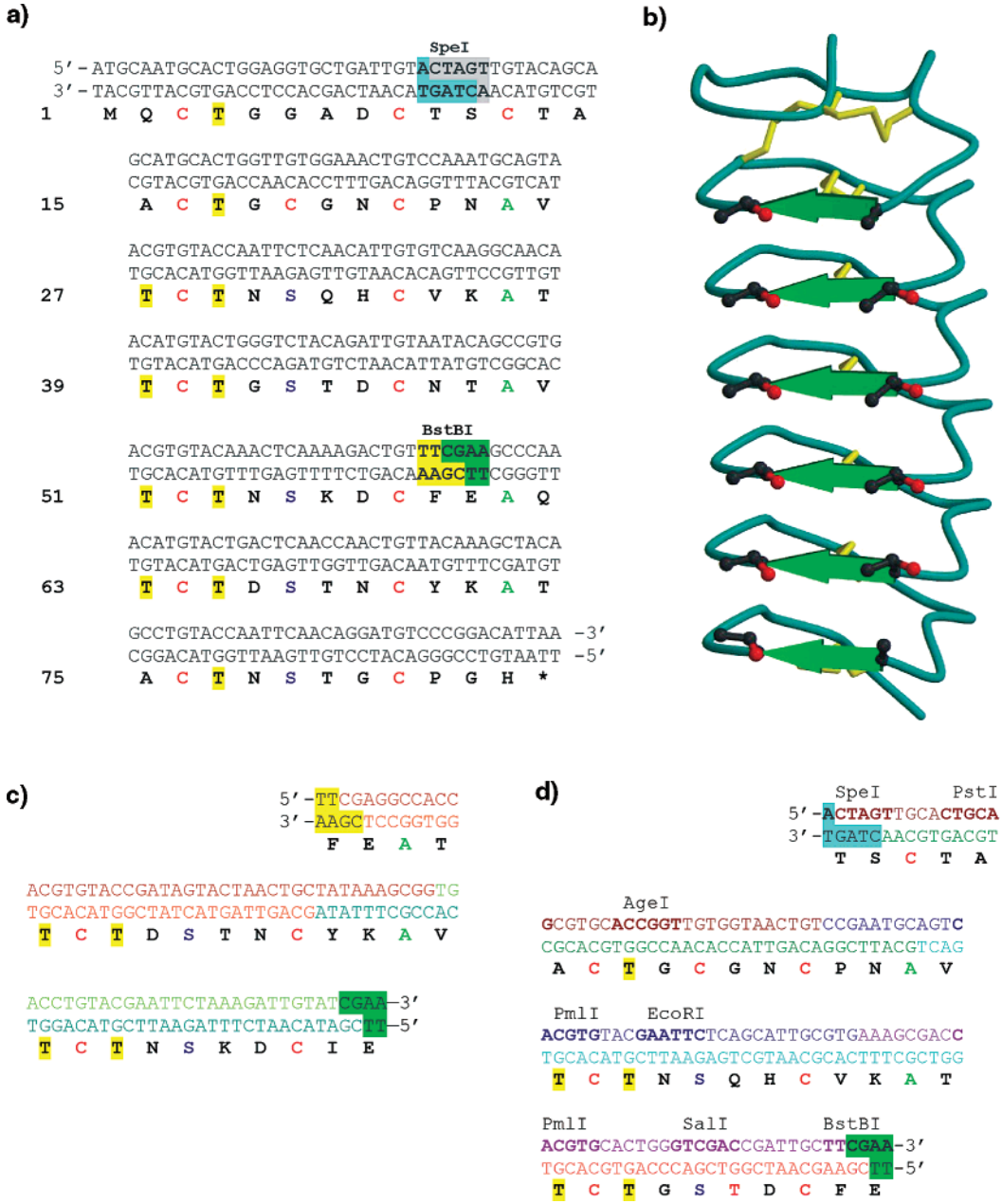

FIGURE 1: Sequence and structure of Tm AFP and engineering strategy. (a) DNA and protein sequences of Tm AFP isoform 4−9 (Tm 4−9). Repetitive amino acids of the consensus coil sequence are colored (Cys in red, Ser in blue, Ala in green, and Thr residues of the Thr array highlighted in yellow). The restriction endonuclease recognition sites that were used to engineer constructs of different lengths are indicated and highlighted with different colors on either side of the cut site. (b) Crystal structure of wild-type Tm AFP (isoform 2−14; *13*) illustrating the ice binding Thr array, disulfide bonds, and β-sheet regions. (c) DNA and protein sequences of the two-coil insertion. Each of the four oligonucleotides that were designed to encode the two-coil insertion sequence is shown in a different color. The overhang allows it to be ligated into the *Bst*BI-digested Tm AFP gene without re-creation of the restriction site. (d) Sequence of the six oligonucleotides (each shown in a different color) and the encoded protein sequence used to produce a Tm AFP variant with one coil removed. The three encoded coils replaced the four coils of the wild-type Tm AFP found between the *Spe*I and *Bst*BI restriction sites. Five new restriction sites (bold) were engineered into this sequence to facilitate further modification of this construct. The generation of a series of constructs containing from 6 to 11 coils using these sequences is described in the text.

With repetitive AFPs, if the repeating structural elements of which they are comprised are viewed as independent ice-binding units, then the total protein size and the surface area of the ice-binding site would be increased in concert by the addition of more of these units to an AFP. Many of the families of repetitive AFP types include isoforms with additional repeats and enhanced activity (*19*).

Most of the type I AFP isoforms produced by winter flounder are comprised of three 11-amino acid tandem repeats and have a mass of ~3.3 kDa. A naturally occurring larger isoform containing four repeats (4.3 kDa) has been isolated from the blood plasma and was found to be considerably more active (~2-fold) than the 3.3 kDa isoforms (*20*). To the other extreme, a synthetic peptide containing just one 11-amino acid repeat from this AFP had no thermal hysteresis activity but still demonstrated ice shaping, indicating that it is able to bind to ice (*21*).

Like the winter flounder, the spruce budworm also carries genes for several isoforms of its β-helical AFPs, most of which encode 9 kDa proteins with six 15-amino acid repeats

(*22*) that together form an array of nine equally spaced Thr residues (*11*). A naturally occurring isoform (501) contains 31 additional amino acids that form two extra loops and is approximately 3 times as active as the shorter isoform (*23*). Excision of the two-loop "insertion" reduces its activity to a level comparable to that of the native 9 kDa proteins.

The beetle *T. molitor* has genes encoding AFP isoforms comprised of seven, eight, or ten tandem repeats of its 12-amino acid consensus repeat sequence (TCTxSxxCxxAx) (*24*). The beetle *Dendroides canadensis* produces homologous isoforms with six or seven repeats (*25*). These repeats form internally disulfide-bonded coils that stack to form the right-handed β-helical structure that presents the ice-binding Thr array. The repetitive structure of Tm AFP provides an ideal opportunity to investigate the relationship between the size and the activity of an AFP. The naturally occurring long isoforms of Tm AFP (e.g., 3−8 and 2−20, with eight and ten coils, respectively) do not form a significant fraction of the AFP found in the hemolymph of the natural host (L. A. Graham, personal communication) and have proven to be difficult to produce by recombinant methods. Nevertheless, the remarkably repetitive β-helical structure and the absence of a hydrophobic core present an "unparalleled" opportunity to engineer AFPs of different lengths to test the relationship between antifreeze activity and ice-binding face surface area. To examine the specific TH activity of Tm AFP variants of a range of sizes, we have generated and tested artificial constructs, based on the seven-coil Tm AFP isoform 4−9, encoding proteins comprised of 6−11 coils.

MATERIALS AND METHODS

Cloning and Expression of Wild-Type Tm 4−9 and a Series of Constructs with a Varying Number of Coils. The cDNA of *T. molitor* AFP isoform 4−9 (Tm 4−9) was cloned into pET 24 (Novagen) between the *Nde*I and *Hin*dIII restriction sites and was expressed in *Escherichia coli* BL21-(DE3) cells as described previously (*15*). Note that isoform 4−9 was used in place of 2−14 (*26*) because it is easier to refold and more tolerant of mutations (*15*). It differs by just five amino acid substitutions.

The cDNA of the seven-coil Tm 4−9 within the expression vector was used as the foundation for the production of the length variants (Figure 1a). To produce Tm 4−9 with two, four, and six additional coils, four oligonucleotides were synthesized (Cortec, Kingston, Canada) to encode both strands of a 24-amino acid sequence (EATTCTDSTNCYKAVTCTNSKDCI) representing two coils of Tm AFP (Figure 1c). The amino acid sequence of these coils conforms to the consensus repeat sequence, and at variable positions (not underlined), amino acids were chosen to introduce stabilizing interactions between their immediate neighbors in adjacent coils. The oligonucleotides were designed such that when annealed, the double-stranded DNA contains single-stranded overhanging ends that are complementary to the cleavage site produced by the restriction endonuclease *Bst*BI (colored yellow and green in Figure 1). The Tm 4−9 construct was cut with *Bst*BI, and the annealed oligonucleotides were added and ligated (T4 ligase) at 15 °C overnight. Upon ligation of this construct into a *Bst*BI site, the two restriction sites are not regenerated. The ligation mixture was therefore digested with *Bst*BI to select against religated vector, and the ligation products were transformed into *E. coli* BL21 by electroporation (Bio-Rad Gene Pulser II). This strategy proved to be highly efficient as clones with one correctly oriented insert, as well as two and three tandemly repeated inserts, encoding proteins with two, four, and six additional coils, were selected.

Minus One, Plus One, and Plus Three Coil Variants. To construct a sequence encoding a Tm 4−9 variant lacking one coil, the 4−9 cDNA in pET 24 was initially digested with *Spe*I and *Bst*BI, to remove a 144 bp sequence (Figure 1a). Three pairs of complementary oligonucleotides were designed to encode the excised sequence, less one coil [the sequence encoding the N^{47}TAVTCTNSKDC^{58} sequence was omitted (Figure 1a,d)]. Again, the sequence to be excised was chosen so that the interactions between the resulting amino acid neighbors on adjacent coils would be favorable, and the synthetic DNA sequence (Figure 1d) was engineered to contain a number of restriction sites for selection and further modification. These oligonucleotides were annealed and ligated into the digested 4−9-containing pET 24 plasmid to create a construct encoding a protein with one fewer coil.

Constructs encoding proteins with one and three additional coils were produced by digesting the "minus one" coil sequence with *Bst*BI and ligating the annealed oligonucleotides that encode two coils (Figure 1c). Clones with one insert and two tandem inserts were selected, encoding proteins with eight and ten coils, respectively. All clones were confirmed by DNA sequencing. Proteins were expressed from pET24 in BL21 cells as described previously (*15*).

Refolding, Protein Purification, and NMR Quality Control. Following expression, the cells were lysed by sonication and the Tm AFPs were allowed to refold in the cell lysate at 4 °C for ∼3 weeks. The thermal hysteresis activity was monitored throughout the refolding process, and when it reached a value of >50% of the expected final activity, oxidized glutathione was added to a final concentration of 25 mM as described previously (*15*). The AFP was then purified by gel permeation chromatography (Sephadex G-75) followed by reversed-phase HPLC (C-18). At this stage of purification, the state of folding of each variant was assessed using one- and two-dimensional nuclear magnetic resonance (NMR) spectroscopy. Samples were prepared by dissolving each protein in 500 μL of a 90% H_2O/10% D_2O mixture (by volume). The pH was adjusted to 6 with microliter aliquots of 100 mM NaOD or DCl as required, and 0.1 mM 2,2-dimethyl-2-silapentane-5-sulfonic acid (DSS) was added as an NMR chemical shift reference. All spectra were acquired at 25 °C on a Varian Unity 600 MHz spectrometer equipped with a 5 mm triple-resonance probe and *z*-axis pulsed field gradients. The experiments included both one-dimensional ^{1}H and two-dimensional ^{1}H homonuclear total correlation spectroscopy (TOCSY) spectra with a mixing time of 54 ms. The spectral width for both dimensions was 7000.4 Hz. The acquired data consisted of 1024 complex data points in the acquisition domain and 256 complex data points in the indirectly detected domain. All NMR spectra were processed using VNMR 6.1B software on a Sun workstation. This revealed that the preparations of all of the variants contained some fraction of unfolded protein.

Ice Affinity Purification. Ice affinity purification (IAP) (*27*) was used to select well-folded proteins and thus ensure that thermal hysteresis assays represented the specific activity of

the properly folded protein only. Briefly, ice was grown slowly from a coldfinger in a solution of AFP. Solutes, including protein impurities and misfolded AFPs, are excluded from this slowly growing mass of ice, whereas functional AFPs adsorb to the ice surface, become overgrown, and are therefore included in the ice. To prepare sufficient quantities of the "plus 2" coil construct for comparison of the starting material with the ice and liquid fractions by two-dimensional NMR, large-scale ice affinity purification was carried out. Approximately 10 mg of HPLC-pure AFP was dissolved in 500 mL of 20 mM ammonium bicarbonate, and an ice hemisphere was grown into this solution using a linear temperature gradient from −0.75 to −4.5 °C over the course of 48 h. Following growth of the hemisphere to 60% of the total volume, the ice and liquid fractions were lyophilized, prepared, and analyzed by NMR spectroscopy in the same manner as the other coil variants previously described. Samples of each of the six protein constructs were prepared for the TH assay on a smaller scale. Lyophilized HPLC-pure samples of each variant (1−5 mg) were dissolved in 30 mL of 20 mM ammonium bicarbonate, and ice growth was achieved with a temperature gradient from −0.5 to −2.5 °C over the course of 20 h. The resulting ice fractions were lyophilized, and stock solutions were prepared by dissolution in water. Series of dilutions for the TH assay were prepared in 100 mM ammonium bicarbonate.

TH Assay. TH activity was assayed using a nanoliter osmometer (Clifton Technical Physics, Hartford, NY) as described previously (*28*) with modifications to accommodate the high activity of insect AFPs (*15*). Briefly, a small drop of an AFP solution is snap-frozen and then melted back to a single crystal. The solution is then slowly cooled until it reaches a temperature at which the ice crystal begins to grow. The difference between this nonequilibrium freezing point and the melting point is the TH activity of the sample. All samples were cooled at a rate of 80 mOsm (0.15 C°) per minute. The TH assays were carried out in triplicate, and the mean and standard deviation are presented, except for the highest concentration of plus 2, as the extremely high TH activity made the assay very difficult and only one reading could be obtained. Protein concentrations were determined by amino acid analysis of stock solutions dissolved in water (Advanced Protein Technology Centre, Hospital for Sick Children, Toronto, ON), and TH assays were carried out in 100 mM NH_4HCO_3.

RESULTS

Protein Expression and Folding. Tm AFP variants with one coil removed and those with one, two, three, and four coils added were expressed at levels comparable to that of wild-type Tm AFP (2−10 mg/L of culture). Following cell lysis, wild-type recombinant Tm AFPs typically exhibit little or no TH activity. They are allowed to refold under mildly oxidizing conditions (exposure to air) for ∼3 weeks to allow the eight disulfide bonds to form correctly (note there are 2×10^6 permutations for disulfide bond formation in Tm AFP isoform 4−9). Surprisingly, the variant with two added coils acquired TH activity more rapidly than the wild type, exhibiting a TH activity of 2100 mOsm after 3 days, at which point wild-type 4−9 typically shows 400−1000 mOsm (1000 mOsm corresponds to 1.86 C° of TH). However, as will be apparent later, part of this activity gain reflects the higher specific activity of the larger construct.

Preparations of wild-type Tm AFP prepared by column chromatography typically contain some protein that is improperly folded. This is represented by a poorly defined broad underlying signal in the "fingerprint" region (8.0−8.5 and 4.0−4.5 ppm) of the two-dimensional ^{1}H TOCSY spectrum that shows correlations of NH protons to α-CH protons (*15*, *26*). This material is extremely difficult to remove, even by reversed-phase HPLC. It has the same mass and charge as the well-folded AFP, and there is essentially no hydrophobic core to help distinguish folded from misfolded forms during reversed-phase chromatography. To assess protein folding, each of the HPLC-pure Tm AFP variants was examined by one- and two-dimensional NMR. The intensities of the diffuse signals in the fingerprint region of the spectra of the HPLC-pure minus 1 and plus 1 coil samples were similar to that seen in the wild-type protein, indicating that an equivalent fraction of protein was unfolded. The constructs with two or more added coils contained significantly more unfolded protein (not shown). Interestingly, the peaks assigned to internal Ser residue peaks are visible as a distinct cluster in each protein's spectrum, and a peak appears or disappears with the addition or excision of each coil (Figure 2). This indicates that each Ser residue of the TCTxSxxCxxAx loop consensus is in a similar chemical environment, which provides evidence that despite the presence of some unfolded protein in each sample, the bulk of the protein is correctly folded.

The presence of unfolded material obscures an accurate comparison between the specific activities of each of the series of variants, as the concentration of well-folded, active AFP is unknown. We have recently demonstrated the purification of AFPs based on antifreeze activity, that is, their ability to bind to ice (*27*). When ice is grown very slowly, solutes including proteins are excluded and "pushed ahead" of the growing lattice. AFPs, however, bind to the surface of ice and become overgrown and incorporated into the ice. We reasoned that misfolded forms of Tm AFPs would lack antifreeze activity and therefore be excluded from ice. Figure 3 illustrates that IAP was remarkably effective at separating well-folded forms from misfolded forms of the Tm AFP variant with two added coils. The original HPLC-pure preparation shows the defined peaks representing well-folded material along with the diffuse region associated with misfolded protein. Following fractionation by ice affinity purification, the ice fraction appears to contain exclusively well-folded protein, while the diffuse signal from misfolded material is present in the liquid fraction only, suggesting that misfolded AFP was excluded from ice. For selection of properly folded AFP before comparison of the TH activities of each of the Tm variants, all preparations were purified by one round of ice affinity purification.

Antifreeze Activity Increases with the Length of the β-Helix. We were interested in determining the extent to which the selection of well-folded AFP using IAP resulted in higher specific TH activity. Figure 4 shows TH activity as a function of protein concentration of HPLC-purified Tm 4−9 versus IAP-pure protein. The well-folded protein purified by IAP exhibits a higher TH activity, although this is only apparent at concentrations of >0.5 mg/mL (60 μM). There is no discernible difference in the early portion of the

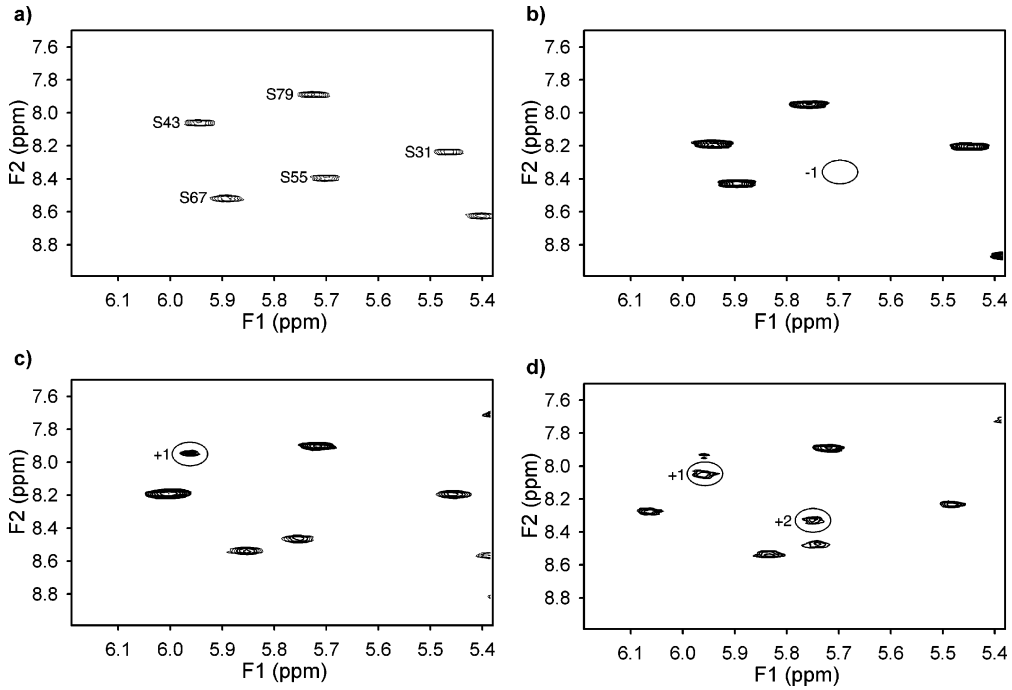

FIGURE 2: Two-dimensional ^{1}H TOCSY NMR spectra of the internal Ser residues of Tm AFP. (a) The wild-type Tm 4−9 spectrum is labeled with the individual peak assignments for the Ser HN−Hα correlations. (b) The location of the deleted Ser peak in the spectra of the minus 1 coil protein is marked. The additional Ser peaks found in (c) the plus 1 coil and (d) the plus 2 coil constructs are indicated.

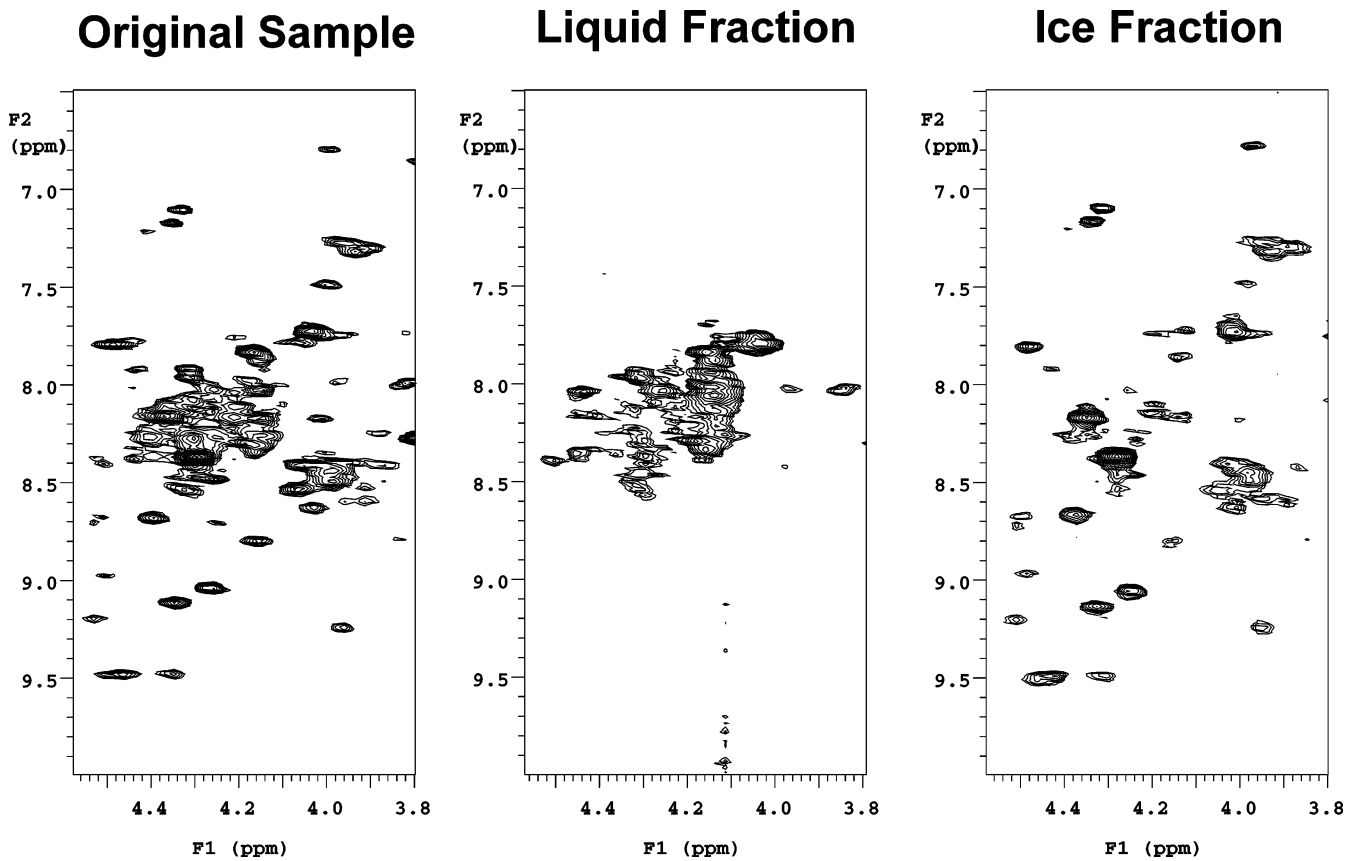

FIGURE 3: Selection of well-folded protein by ice affinity purification. Two-dimensional ^{1}H TOCSY NMR spectra of the fingerprint region (3.8−4.5 and 6.5−10 ppm) are shown for three samples: the "original" HPLC-pure material and the ice and liquid (excluded from ice) fractions following ice affinity purification. This region represents correlations of NH protons with α-CH protons where clear sharp peaks indicate well-folded material and broad undefined peaks are indicative of misfolded random coil.

curve where the gain in activity as a function of AFP concentration is particularly steep.

The activity plot of wild-type Tm 4−9 is similar to that seen previously (*15*, *26*). The relationship between TH and [AFP] appears to be hyperbolic, with 4 C° of TH obtained at 1.5 mg/mL (180 μM). The removal of one coil causes a dramatic 4-fold loss of activity across the concentration range (Figure 5a). It is worth noting that this activity is still 5−10-

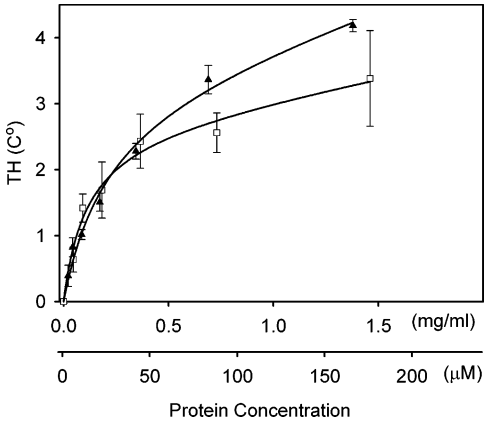

FIGURE 4: Ice affinity purification increases the specific activity of Tm AFP. Thermal hysteresis activity as a function of concentration (shown in micromolar and milligrams per milliliter) for wild-type Tm 4−9 purified by HPLC (□) or by HPLC followed by ice affinity purification (▲).

fold greater than that achieved by fish AFPs. The addition of two loops produces an equally dramatic gain in activity. This is particularly apparent at very low AFP concentrations. Above 4 C°, the gain in activity enters a second phase with a decreasing slope, but shows no sign of reaching a plateau activity. It is difficult to read activities above 6−6.5 C° using the Clifton nanoliter osmometer. The activity curve for "plus 1" is intermediate between those of the wild type and plus 2. It shows a proportionally rapid increase in activity that is intermediate between those of the larger and smaller members of the series, but it tapers off more than the others and appears to approach a plateau value.

The relationship between TH activity and AFP concentration is nonlinear, and the difference in AFP activities is not strictly proportional over the concentration range. Nevertheless, it is instructive to compare the activity of different AFPs at one concentration. At 60 μM, the removal of one coil from Tm AFP decreased its activity by almost 5-fold (4.7), while adding one coil increased the activity by 1.6-fold (Figure 6b). The most highly active protein in this series was produced by the addition of two coils, which more than doubled (2.2-fold) the TH activity.

In addition to comparing the TH activity of each construct at a fixed concentration, we have compared the concentration of each construct that is required to produce a given TH activity (Figure 6c). A concentration of ~28 μM of IAP-pure wild-type Tm 4−9 is required for a TH activity of 2 C°. When one coil is removed, a 16-fold higher concentration (460 μM) is required to exert the same activity. However, when one coil is added, 2 C° of TH can be realized by a 4-fold lower concentration (7 μM). Remarkably, the addition of two coils produces an AFP that reaches 2 C° of TH with a concentration of only 0.9 μM, 32-fold lower than that required by the wild-type protein.

The comparisons described above are made using molar concentrations; however, if compared on a milligram per milliliter basis, these differences are only slightly less pronounced (Figure 5b). Compared on a milligram per milliliter basis, the two-coil insert enhances activity by 25-fold: 2 C° of TH is produced by 0.01 mg/mL versus 0.25 mg/mL for the wild type.

Law of Diminishing Returns Applied to AFP Length. The trend of increasing specific activity with extra coils did not

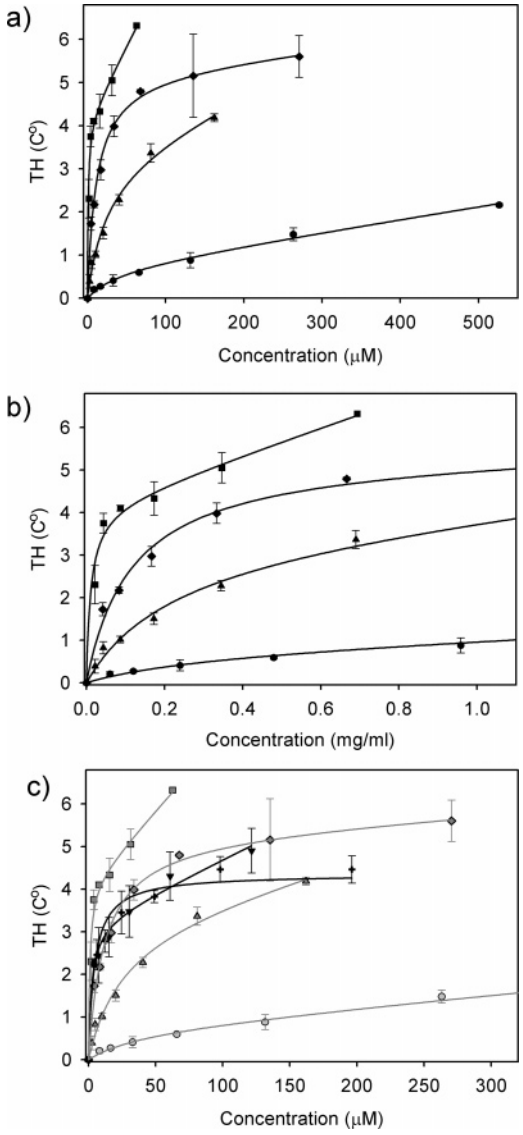

FIGURE 5: Relationship between the thermal hysteresis activity and size of the Tm AFP construct. (a) Thermal hysteresis activity as a function of concentration (micromolar) for wild-type Tm 4−9 (▲), Tm AFP minus one coil (●), Tm AFP plus one coil (◆), and Tm AFP plus two coils (■). (b) Thermal hysteresis activity as a function of concentration on a milligrams per milliliter basis for the same four constructs, with the low-concentration region expanded. (c) Thermal hysteresis of Tm AFP plus three coils (○) and plus four coils (+) superimposed over the activity curves of the other four constructs, which are shown in gray.

continue with the addition of three and four coils. These constructs were less active than the plus 2 protein, demonstrating specific activities like the construct with one additional coil (Figure 5c). It is interesting to note that the shape of the TH standard curves changes as the size of the proteins increases. The minus 1 loop curve is a very shallow hyperbola, which is not far from linearity, whereas the wild-type curve more closely resembles a "classic" hyperbola. As more loops are added to the AFPs, the hyperbolic shapes of the TH curves become more rectangular. In general, the larger proteins exhibit high activities at low concentrations; however, the activities approach a plateau earlier. For example, the plus 1, plus 3, and plus 4 coil AFPs have comparable TH activities; however, at low concentrations (<30 μM), the plus 4 coil variant has the highest activity,

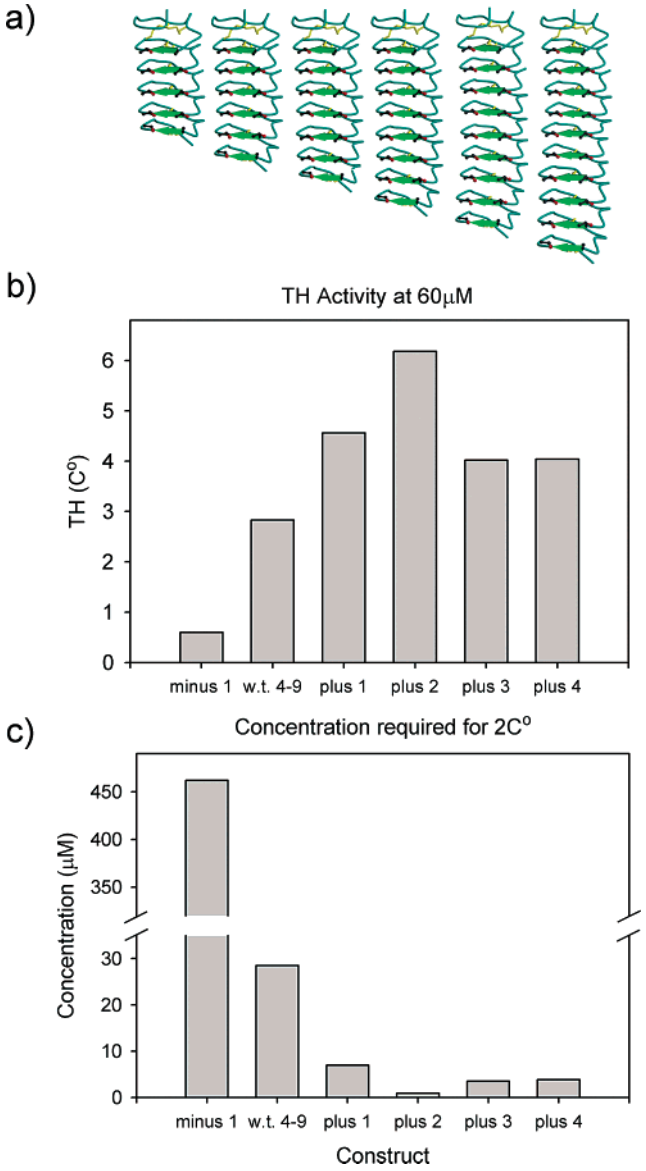

FIGURE 6: Comparison of the specific activities of Tm AFP constructs with a variable number of coils. (a) Representation of the relative sizes of Tm AFP variants (minus 1 coil to plus 4 coils) based on the crystal structure of Tm 2−14. (b) Comparison of the thermal hysteresis activity produced by each of the constructs at a concentration of 60 μM. (c) Comparison of the concentration (micromolar) of each construct that is required to produce 2 C° of thermal hysteresis.

closely followed by plus 3. With an increase in concentration, however, the activity of the plus 4 construct begins to plateau, and at concentrations between 40 and 120 μM, the plus 1 construct has the highest activity of these three proteins. At ~160 μM, the activity of the wild-type protein is as high as that of the plus 4 construct.

All of the Tm AFP variants produced the same symmetrical lemon-shaped ice crystal morphology (*29*). However, highly active samples (>4 C°) were more likely to produce amorphous or rough ice crystals that tended to retain the characteristics of the melting seed rather than "filling out" to the lemon shape.

To try to establish the minimum number of repeats necessary to effect TH activity, a variant of Tm AFP with two loops excised was also produced. This construct expressed well in *E. coli* and could be purified in reasonable quantities, but had little or no TH activity (20 mOsm at ~5 mg/mL). Upon examination by NMR, this sample produced no sign of a well-folded protein. A construct with six additional loops was also successfully cloned and expressed, albeit in very small quantities. The specific activity of this variant was substantially lower than that of the plus 4 coil protein. Because quantities were limited and TH activity was poor, we did not pursue ice affinity purification and amino acid analysis to establish an accurate standard activity curve.

DISCUSSION

The unique structure of the right-handed β-helical beetle AFP has provided an ideal opportunity to systematically vary its length and hence the area of the ice binding surface to examine how this affects antifreeze activity. In particular, the extreme regularity of the helix, with its internally disulfide-bonded 12-amino acid coil and the absence of a hydrophobic core, has made this a relatively straightforward protein engineering project. This AFP was chosen as a template for designing and producing a continuous series of AFP variants comprised of varying numbers of coils. The repetitive sequence and structure suggested that each coil might act as an independent ice-binding module and that the fold might tolerate the insertion and excision of coils. The inserted coils were based on the 12-amino acid consensus sequence with residues for the variable positions selected to form stabilizing pairs across β-sheets, such as salt bridges (EK), hydrophobic "stacks" (FY), and Asx "ladders" (DN). These types of stabilizing features are observed in the crystal structure of Tm AFP (*13*). The wild type and five variants were well-expressed, and sufficient quantities of well-folded proteins were obtained by IAP.

Analysis of TH activity as a function of concentration (Figure 5a−c) demonstrates that the activity of Tm AFP constructs changes dramatically with the number of coils. Excising one coil reduces TH activity to less than one-quarter of that of the wild type, whereas the addition of two coils doubles the TH activity and allows the AFP to reach a given TH with an ~30-fold lower concentration. The enhancement of activity with increasing size reaches an upper limit and does not continue with the further insertion of coils. In fact, the additional coils in the plus 3 and plus 4 constructs reduce activity to below that of the plus 2 construct.

The increase in activity with added repeats is consistent with general observations made over the years about natural AFP isoforms. The four-repeat type I isoform AFP-9 (*20*) is ~33% larger than the three-repeat isoform HPLC-6. The entire length of the α-helix is thought to interact with ice, and therefore, the surface area of the ice-binding face of AFP-9 is also 33% greater. This relatively modest size increase roughly doubles the specific TH activity. Sbw AFP isoform 501 is comprised of eight β-helical loops, whereas isoform 337 contains six loops, making the total size of 501 again ~33% larger. Isoform 337 contains five of the TXT motifs that are thought to mediate binding to ice, whereas isoform 501 contains seven, although three are imperfect and have Thr to Ile substitutions. This suggests that the functional ice binding surface area of 501 is as much as 40% larger. Remarkably, this modest increase in size makes the 501 isoform ~3-fold more active than the 337 isoform (*23*). While both of these results are remarkably consistent with

the current results, the range of AFP size is limited in each case to the naturally occurring isoforms. Furthermore, interpretation of the results is subject to the possibility that the differences in TH activity between the isoforms of type I and sbw AFP may be influenced not only by length but also by variation in sequence. This seems particularly likely for sbw 501 in view of the amino acid substitutions on the ice-binding face. In this study, the engineering of Tm AFP variants allowed the production of AFPs of continuously variable size with highly conserved sequence. Because these engineered variants are based on a common core structure, they provide a more controlled and complete examination of the relationship between size and activity.

However, since each coil of Tm AFP contains a TXT ice-binding motif, the addition of coils increases both the total size of the protein and the area of the ice-binding face. A series of fusion proteins of the globular type III AFP indicate that increasing either the total protein size or the ice binding surface area contributes to TH activity, but that the latter is far more important. The fusion of a functional type III AFP to a second inactivated version that contains a steric mutation on the ice-binding face produced a small (20%) enhancement in activity. However, a "dimer" produced by linking two functional type III domains in tandem via a flexible linker that allows the ice-binding faces of each subunit to simultaneously dock to the ice surface doubled the TH activity (*30*). An extension of this approach in which six AFP domains are linked in tandem produces an even greater increase in activity (*31*). However, if two functional AFPs were linked by a disulfide bond in an orientation that does not allow the two ice-binding faces to adsorb to the ice surface at the same time, the TH activity increased by only 20%, as with the fusion to the inactive domain. The activity of an AFP fusion protein seems to vary with the size of the fused domain, and it is possible to double the activity of type III AFP by connecting it to maltose-binding protein (42 kDa), which increases its size 7-fold (*18*).

Thus, while increasing the total size of an antifreeze protein can enhance activity, increasing the surface area of the ice-binding face does so much more dramatically. Increasing the ice binding surface area by ~33% can enhance TH activity to a degree equal to or greater than a 7-fold increase in total protein size.

Preparations of Tm AFP purified by conventional methods produce NMR spectra that contain some undefined signals in the fingerprint region, revealing the copurification of misfolded forms. We have previously been unable to remove this material using chromatography, although it could be minimized at the HPLC step at the expense of drastically reduced yields. Fortunately, IAP has proven to be remarkably effective for the purification of well-folded AFP and, as predicted, the specific TH activity increases following IAP, presumably because a greater fraction of the protein is well-folded and active. We have speculated that the undefined fingerprint represents a fraction of the molecules of protein that are misfolded, as opposed to part of each protein molecule that is flexible (*15*, *26*). This is supported by the ability of IAP to separate the protein that produces defined signals indicative of well-folded material from the unfolded material that produces undefined spectra.

The most active Tm AFP variant, with two extra loops, has six TXT motifs displayed on β-sheets flanked by coils with AXT sequences. There are a few plausible explanations for why the addition of extra coils does not enhance activity any further. First, the spacing between β-strands on the ice-binding face of Tm AFP makes a close yet imperfect match to the spacing of the ice lattice. Tm AFP is hypothesized to bind to both the prism and basal planes of ice, each of which exhibits a 4.52 Å spacing between O atoms that is closely matched by the spacing between the β-sheets of the protein. On the basis of the crystal structure of Tm 2−14 [Protein Data Bank entry 1EZG (*13*, *26*)], the average spacing between the β-carbon atoms of the Thr residues in the long rank (the left side in Figure 1b) of the ice-binding face of wild-type Tm AFP is 4.70 Å and on the shorter rank (right side) this spacing is 4.85 Å. The difference of 0.15 Å results in a slight angle between adjacent β-strands that introduces a minor bend into the ice-binding face of Tm AFP. There is also a mismatch of 0.18−0.33 Å between the spacing of the β-strands and that of the ice lattice. Because this mismatch is cumulative with each added strand, there is a limit to the number of parallel β-strands that can simultaneously align (from a static structure) with the ice lattice and contribute to binding. Furthermore, the bend in the helix that is caused by the angle between β-strands would become more pronounced with the addition of coils. This bend in the AFP would cause added TXT motifs to be even more poorly aligned with the ice lattice. Misaligned ice binding surface residues would not contribute to ice binding, and may cause steric interference, decreasing the probability that the AFP will successfully bind to ice. In the ensemble of 20 NMR structures of Tm AFP in solution [Protein Data Bank entry 1L1I (*14*)], a bend in the helix is apparent in virtually all of the structures, indicating that this is not an artifact of crystallization. The average distance between each pair of Thr β-carbons on the ice-binding face in all 20 structures is 5.23 Å, clearly indicating a poorer match to ice. However, there is considerable variation within the ensemble of structures, and most of the pairs can be found at a spacing that makes a good match to ice in some of the structures, suggesting a degree of "induced fit". It is likely that the large constructs are less rigid than the wild-type AFP and that such flexible proteins would bind ice more poorly due to reduced surface−surface complementarity and entropic penalties. These longer constructs might be more susceptible to larger, slower-scale bending motion across the *z*-axis of the β-helix in the direction of the observed curve in the structure.

Tm AFP and sbw AFP are similar in size and produce similar TH activities. The addition of two loops to each protein increases the surface area of the ice-binding face by a similar factor (~40%), but this triples the activity of sbw AFP and only doubles the activity of Tm AFP. sbw AFP may exhibit a larger increase in specific activity with added loops because it makes a better match to the ice lattice spacing. In the 501 isoform, the average spacing between Thr β-carbons on adjacent strands in the more "conserved" rank is 4.63 Å, which matches the ice lattice with a deviation of only 0.11 Å. Furthermore, this protein does not bend as Tm AFP does, as the spacing on the less conserved side, which contains Ile and Val substitutions, is on average 4.65 Å. It is interesting to speculate that the activity of sbw AFP might continue to increase with the addition of more loops. Unfortunately, the structure of this AFP makes it less amenable to a similar protein engineering project. The

consensus sequence of its loops is considerably more variable, and the internal side chains form an intricately packed hydrophobic core. Furthermore, the disulfide bonds that stabilize sbw AFP do not form within coils as with Tm AFP, but form between adjacent loops, limiting the use of individual loops as repetitive structural elements.

The results of this study, together with the remarkably similar findings with other AFPs, raise the question of why a small increase in the ice binding surface area of an AFP can cause such a profound increase in TH activity. It is tempting to ascribe the increased activity to an enhanced affinity for ice; however, the generally accepted "irreversible binding" hypothesis predicts that all AFPs must bind to ice irreversibly (*32*). If there were any appreciable off-rate, the ice would slowly grow behind the AFPs as they dissociate. The hypothesis that all wild-type AFPs bind ice with similar affinity is supported by the observation that fish and insect AFPs, despite their 10−100-fold difference in TH activity, partition similarly into a growing ice mass (*33*). If the density of AFPs bound to the surface of ice is directly related to the molar AFP concentration, then at a given concentration, the accessible surface between AFPs would decrease as the size of the AFPs increases. Thus, the growth of ice would be confined to a smaller radius of curvature, which would lead to higher TH activity by the Kelvin effect. However, because the proportional change in this radius would be larger when the AFPs are closer together, the effect on TH of increasing the size of an AFP should be more apparent at high concentrations. The results are not consistent with this reasoning, as the enhancement of AFP activity with increasing size is most dramatic at low concentrations. Perhaps high AFP concentrations are needed to control weak points, like junctions between planes, whereas 99% of the crystal surface might be well "protected" at low AFP concentrations.

The spectacularly high TH activity of the Tm 4−9 variant with the engineered addition of two loops has considerable potential for biotechnological applications. It can provide the same degree of freeze protection as wild-type AFP at a 30-fold lower concentration. This could be invaluable in the production of transgenic plants (*34*) or animals (*35*) where the levels of protein expression are often limited by a low copy number of the transgene.

By extrapolation from Figure 5a, the maximal TH activity of the plus 2 construct is likely approximately twice that of the wild type, which could allow a transgenic organism with high expression levels to survive in environments several degrees colder than would be possible with expression of wild-type Tm AFP. Furthermore, this construct appears to fold *in vitro* more rapidly than the wild-type protein, suggesting that it could be produced on an industrial scale somewhat more efficiently for biotechnological applications (*36*−*38*).

CONCLUSIONS

To investigate the relationship between TH activity and the size of the ice-binding face of an AFP, we have exploited the repetitive nature of the β-helical AFP from *T. molitor*. We produced a series of constructs that vary in the number of repeating subunits that form the helical coils, and isolated well-folded protein by its affinity for ice. The specific TH activity of Tm AFP was dramatically reduced by the deletion of one coil, but increased with added coils up to a maximum that was achieved by inserting two coils to form a nine-coil AFP. This engineered AFP was more than twice as active as the wild type when compared at the same molar concentration, and matched wild-type activity with a >30-fold lower concentration. TH activity could not be further enhanced via addition of more coils, presumably due to an imperfect match to the ice lattice and increased conformational flexibility.

REFERENCES

1. Fletcher, G. L., Hew, C. L., and Davies, P. L. (2001) Antifreeze proteins of teleost fishes, *Annu. Rev. Physiol. 63*, 359−390.
2. Duman, J. G. (2001) Antifreeze and ice nucleator proteins in terrestrial arthropods, *Annu. Rev. Physiol. 63*, 327−357.
3. Atici, O., and Nalbantoglu, B. (2003) Antifreeze proteins in higher plants, *Phytochemistry 64*, 1187−1196.
4. Yeh, Y., and Feeney, R. E. (1996) Antifreeze Proteins: Structures and Mechanisms of Function, *Chem. Rev. 96*, 601−618.
5. Ewart, K. V., Lin, Q., and Hew, C. L. (1999) Structure, function and evolution of antifreeze proteins, *Cell. Mol. Life Sci. 55*, 271−283.
6. Jia, Z., and Davies, P. L. (2002) Antifreeze proteins: an unusual receptor−ligand interaction, *Trends Biochem. Sci. 27*, 101−106.
7. Davies, P. L., Baardsnes, J., Kuiper, M. J., and Walker, V. K. (2002) Structure and function of antifreeze proteins, *Philos. Trans. R. Soc. London, Ser. B 357*, 927−935.
8. Raymond, J. A., and DeVries, A. L. (1977) Adsorption inhibition as a mechanism of freezing resistance in polar fishes, *Proc. Natl. Acad. Sci. U.S.A. 74*, 2589−2593.
9. Wilson, P. W. (1993) Explaining thermal hysteresis by the Kelvin effect, *Cryo-Lett. 14*, 31−36.
10. Baardsnes, J., Kondejewski, L. H., Hodges, R. S., Chao, H., Kay, C., and Davies, P. L. (1999) New ice-binding face for type I antifreeze protein, *FEBS Lett. 463*, 87−91.
11. Graether, S. P., Kuiper, M. J., Gagne, S. M., Walker, V. K., Jia, Z., Sykes, B. D., and Davies, P. L. (2000) β-Helix structure and ice-binding properties of a hyperactive antifreeze protein from an insect, *Nature 406*, 325−328.
12. Leinala, E. K., Davies, P. L., and Jia, Z. (2002) Crystal structure of β-helical antifreeze protein points to a general ice binding model, *Structure 10*, 619−627.
13. Liou, Y. C., Tocilj, A., Davies, P. L., and Jia, Z. (2000) Mimicry of ice structure by surface hydroxyls and water of a β-helix antifreeze protein, *Nature 406*, 322−324.
14. Daley, M. E., Spyracopoulos, L., Jia, Z., Davies, P. L., and Sykes, B. D. (2002) Structure and Dynamics of a β-Helical Antifreeze Protein, *Biochemistry 41*, 5515−5525.
15. Marshall, C. B., Daley, M. E., Graham, L. A., Sykes, B. D., and Davies, P. L. (2002) Identification of the ice-binding face of antifreeze protein from *Tenebrio molitor*, *FEBS Lett. 529*, 261−267.
16. Ewart, K. V., Rubinsky, B., and Fletcher, G. L. (1992) Structural and functional similarity between fish antifreeze proteins and calcium-dependent lectins, *Biochem. Biophys. Res. Commun. 185*, 335−340.
17. Baardsnes, J., and Davies, P. L. (2001) Sialic acid synthase: the origin of fish type III antifreeze protein? *Trends Biochem. Sci. 26*, 468−469.
18. DeLuca, C. I., Comley, R., and Davies, P. L. (1998) Antifreeze proteins bind independently to ice, *Biophys. J. 74*, 1502−1508.
19. Feeney, R. E., Burcham, T. S., and Yeh, Y. (1986) Antifreeze glycoproteins from polar fish blood, *Annu. Rev. Biophys. Biophys. Chem. 15*, 59−78.
20. Chao, H., Hodges, R. S., Kay, C. M., Gauthier, S. Y., and Davies, P. L. (1996) A natural variant of type I antifreeze protein with four ice-binding repeats is a particularly potent antifreeze, *Protein Sci. 5*, 1150−1156.
21. Houston, M. E., Jr., Chao, H., Hodges, R. S., Sykes, B. D., Kay, C. M., Sonnichsen, F. D., Loewen, M. C., and Davies, P. L. (1998) Binding of an oligopeptide to a specific plane of ice, *J. Biol. Chem. 273*, 11714−11718.
22. Doucet, D., Tyshenko, M. G., Kuiper, M. J., Graether, S. P., Sykes, B. D., Daugulis, A. J., Davies, P. L., and Walker, V. K. (2000)

Structure−function relationships in spruce budworm antifreeze protein revealed by isoform diversity, *Eur. J. Biochem. 267*, 6082−6088.
23. Leinala, E. K., Davies, P. L., Doucet, D., Tyshenko, M. G., Walker, V. K., and Jia, Z. (2002) A β-helical antifreeze protein isoform with increased activity. Structural and functional insights, *J. Biol. Chem. 277*, 33349−33352.
24. Liou, Y. C., Thibault, P., Walker, V. K., Davies, P. L., and Graham, L. A. (1999) A complex family of highly heterogeneous and internally repetitive hyperactive antifreeze proteins from the beetle *Tenebrio molitor*, *Biochemistry 38*, 11415−11424.
25. Li, N., Kendrick, B. S., Manning, M. C., Carpenter, J. F., and Duman, J. G. (1998) Secondary structure of antifreeze proteins from overwintering larvae of the beetle *Dendroides canadensis*, *Arch. Biochem. Biophys. 360*, 25−32.
26. Liou, Y. C., Daley, M. E., Graham, L. A., Kay, C. M., Walker, V. K., Sykes, B. D., and Davies, P. L. (2000) Folding and structural characterization of highly disulfide-bonded beetle antifreeze protein produced in bacteria, *Protein Expression Purif. 19*, 148−157.
27. Kuiper, M. J., Lankin, C., Gauthier, S. Y., Walker, V. K., and Davies, P. L. (2003) Purification of antifreeze proteins by adsorption to ice, *Biochem. Biophys. Res. Commun. 300*, 645−648.
28. Chakrabartty, A., and Hew, C. L. (1991) The effect of enhanced α-helicity on the activity of a winter flounder antifreeze polypeptide, *Eur. J. Biochem. 202*, 1057−1063.
29. Graham, L. A., Liou, Y. C., Walker, V. K., and Davies, P. L. (1997) Hyperactive antifreeze protein from beetles, *Nature 388*, 727−728.
30. Baardsnes, J., Kuiper, M. J., and Davies, P. L. (2003) Antifreeze protein dimer: when two ice-binding faces are better than one, *J. Biol. Chem. 278*, 38942−38947.
31. Nishimiya, Y., Ohgiya, S., and Tsuda, S. (2003) Artificial multimers of the type III antifreeze protein. Effects on thermal hysteresis and ice crystal morphology, *J. Biol. Chem. 278*, 32307−32312.
32. Knight, C. A., and DeVries, A. L. (1994) Effects of a polymeric, nonequilibrium 'antifreeze' upon ice growth from water, *J. Cryst. Growth 143*, 301−310.
33. Marshall, C. B., Tomczak, M. M., Gauthier, S. Y., Kuiper, M. J., Lankin, C., Walker, V. K., and Davies, P. L. (2004) Partitioning of fish and insect antifreeze proteins into ice suggests they bind with comparable affinity, *Biochemistry 43*, 148−154.
34. Huang, T., Nicodemus, J., Zarka, D. G., Thomashow, M. F., Wisniewski, M., and Duman, J. G. (2002) Expression of an insect (*Dendroides canadensis*) antifreeze protein in *Arabidopsis thaliana* results in a decrease in plant freezing temperature, *Plant Mol. Biol. 50*, 333−344.
35. Hew, C., Poon, R., Xiong, F., Gauthier, S., Shears, M., King, M., Davies, P., and Fletcher, G. (1999) Liver-specific and seasonal expression of transgenic Atlantic salmon harboring the winter flounder antifreeze protein gene, *Transgenic Res. 8*, 405−414.
36. Amir, G., Rubinsky, B., Horowitz, L., Miller, L., Leor, J., Kassif, Y., Mishaly, D., Smolinsky, A. K., and Lavee, J. (2004) Prolonged 24-hour subzero preservation of heterotopically transplanted rat hearts using antifreeze proteins derived from arctic fish, *Ann. Thorac. Surg. 77*, 1648−1655.
37. Amir, G., Rubinsky, B., Kassif, Y., Horowitz, L., Smolinsky, A. K., and Lavee, J. (2003) Preservation of myocyte structure and mitochondrial integrity in subzero cryopreservation of mammalian hearts for transplantation using antifreeze proteins: an electron microscopy study, *Eur. J. Cardiothorac. Surg. 24*, 292−297.
38. Griffith, M., and Ewart, K. V. (1995) Antifreeze proteins and their potential use in frozen foods, *Biotechnol. Adv. 13*, 375−402.

BI0488909